Vacuum 115 (2015) 19–22

Contents lists available at ScienceDirect

Vacuum

journal homepage: www.elsevier.com/locate/vacuum

Rapid communication

Scanning transmission electron microscopy technique for morphology analysis of anodic oxide film formed on titanium

Z. Liu [a, *], T. Hashimoto [a], I.-Ling Tsai [b], G.E. Thompson [a], P. Skeldon [a], H. Liu [a]

[a] Corrosion & Protection Centre, School of Materials, The University of Manchester, M13 9PL, UK
[b] Oxford Instruments NanoAnalysis, HP12 3SE High Wycombe, UK

ARTICLE INFO

Article history:
Received 5 January 2015
Received in revised form
21 January 2015
Accepted 27 January 2015
Available online 7 February 2015

Keywords:
STEM-in-SEM
Anodic oxide film
Titanium
6-specimen carousel holder

ABSTRACT

The application of scanning transmission electron microscopy for morphological observation of anodic oxide films formed on titanium has been successfully explored. Important details of anodic films are readily recorded from high quality images by scanning transmission electron microscopy, which enabled the study of the film morphology, identification of film thickness and the presence of oxygen bubble features. By combining the large field of view with flexible magnification ranges in the scanning transmission electron microscopy, it was possible to study the morphology of the oxide film. A 6-specimen carousel holder would provide an increase in productivity by ~20% compared with a conventional, single-specimen scanning transmission electron microscopy or transmission electron microscopy.

The use of anodized titanium in an increasing range of applications has resulted in a growing demand for detailed information on the morphology of the anodic films in order to derive crystalline structure – property correlations. In the microstructure analysis of anodic oxide films, the structure and occurrence of oxygen evolution are examined to precise a deep understanding of the coating performance. This is also critical for optimization of the titanium surface and processing conditions for specific requirements in the aerospace industries [1–3].

Transmission electron microscopy (TEM) is the most frequently used technique for the study of the morphology of thin film coatings. The TEM technique, however, presents some limitations: the equipment is expensive; the analysis is time-consuming and is somewhat skill-intensive. Recently, some publications have reported the value of the scanning transmission electron microscopy in scanning electron microscopy (STEM-in-SEM) technique in the areas of mineralogy and petrology [4], semiconductors [5], nanomaterials [6,7], polymers and catalysts [8]. The STEM-in-SEM has been shown to be a rapid and easy method for characterization of the morphology and the internal structure of mineral and rock specimens, and it was shown to be particularly useful in microbiology research [9]. In addition, an exhaustive high-resolution STEM-in-SEM study of laser-machined silicon structures was carried out to characterize defects in the crystal lattice, thermal-mechanical damage, internal structure, compositions, and dimensions of the laser-machined structures [10].

However, according to the authors' knowledge, studies of anodic oxide film growth on titanium using an STEM-in-SEM technique have not been reported in any previous research. Thus, in the present work, the application of STEM-in-SEM to anodic oxide films formed on titanium is demonstrated. Some examples of anodic films formed on titanium are presented, with emphasis on the film morphology and oxygen bubble features etc., which are routinely probed by TEM.

A Zeiss Ultra 55 scanning electron microscopy, equipped with a scanning transmission electron microscopy detector was used in the present study. The schematic diagrams of Fig. 1 show a 6-specimen carousel holder and its rotation direction. Within the SEM chamber, the STEM detector unit consists of the detector and an extension arm for the adjustment of the X, Y and Z directions. The extension arm also carries the detector back and forth between a “rest” position and an “active” position when imaging. In the “active” imaging mode, the 6-specimen carousel holder is used and the STEM detector is perfectly aligned. In the “rest” mode, the detector is “parked” away by simply retracting the detector to a safe distance. Also, if the detector is not “parked” away, the joystick function is used to freeze it during the “active” mode in order to protect the STEM detector and, when in the “rest” mode, the

* Corresponding author. Tel.: +44 07873507226.
E-mail address: zuojia.liu@gmail.com (Z. Liu).

http://dx.doi.org/10.1016/j.vacuum.2015.01.027
0042-207X/

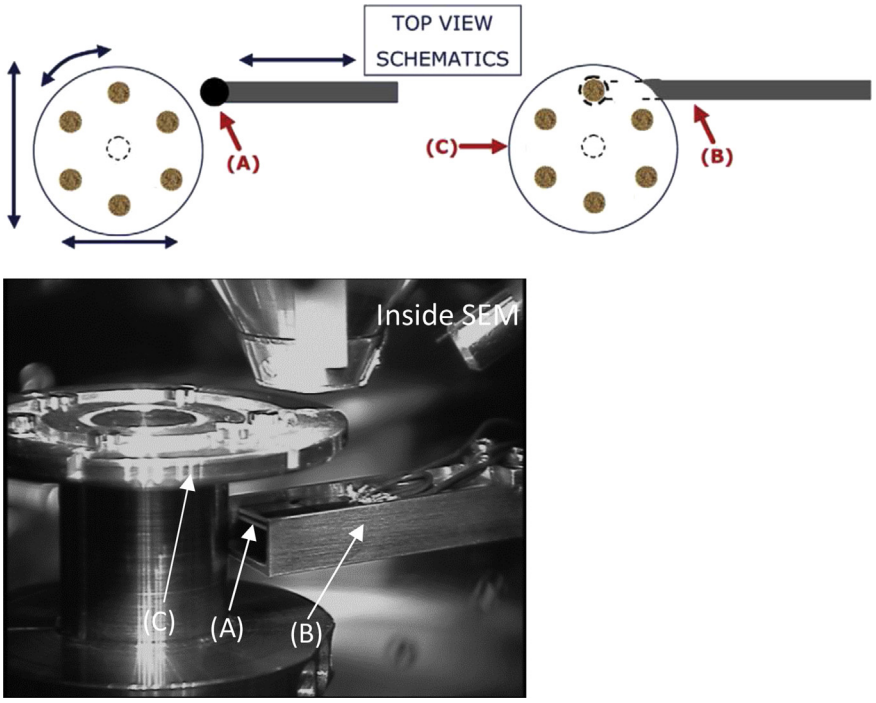

Fig. 1. Photo inside the SEM chamber corresponds to the schematics of the top view of parts (A), (B) and (C), represent for STEM detector, detector extension arm and carousel holder; The 6-specimen carousel is aligned with the electron column; the STEM detector is controlled with the detector arm to back and forth, and the adjustment of X, Y and Z directions; the imagining is ready after the working distance is set for both carousel holder and STEM detector.

joystick is released and controlled to change the position of the grid holder. STEM-in-SEM evaluations were conducted at an operating acceleration voltage of 30 kV in order to improve the electron penetration and the brightness of the source with an optimized working distance of 4 mm.

99.9% pure aluminium foils, of dimensions of 4.0 × 2.0 cm, were electropolished at 20 V for 3 min in a 4 to 1 by vol. mixture of ethanol/perchloric acid at a temperature of 278 K. After electropolishing, the specimens were rinsed in ethanol and deionized water, and dried in a cool air stream. DC magnetron sputtering was carried out on electropolished aluminium substrates using an Oxford Applied Research system, with a 99.6% titanium target of 50 mm diameter. The system was first evacuated to a vacuum condition of 1×10^{-7} Pa, with subsequent deposition from the titanium source at 300 mA in a 99.99% argon atmosphere at 0.5 Pa for 60 min, and a sputter-deposited titanium layer of ~120 nm thickness was obtained. The finished specimens were masked with lacquer 45 to leave an exposed region of dimensions of 1.0 × 1.0 cm for the subsequent anodizing treatment. Individual specimens were anodized at 50 V in 1 M phosphoric acid for 900 s with continuous stirring at ambient temperature. A sheet of pure aluminium, of size 8 × 10 cm, was used as the cathode. The current density − time response was recorded electronically, employing a Labview data acquisition system (National Instruments). After anodizing, the specimen was rinsed with deionized water and dried in a cool air stream. In order to generate thin transparent specimens, a nominally 15 nm thickness of the specimen was prepared using a Leica EM UC7 instrument of ultramicrotomy at a cutting speed of 0.15 mm s^{-1}. The section slices were floated on water behind the diamond knife, and collected on standard TEM mesh copper grids.

Fig. 2 compares images of the ultramicrotomed sections in the SE mode and STEM mode at a very low magnification. The difference in contrast between these selected two modes is evident. It is known that the SE mode detection is operated by secondary electrons emitted by atoms which are excited by the electron beam [11]. Then, by scanning the specimen and detecting the secondary electrons, an image displaying the topography of the surface is

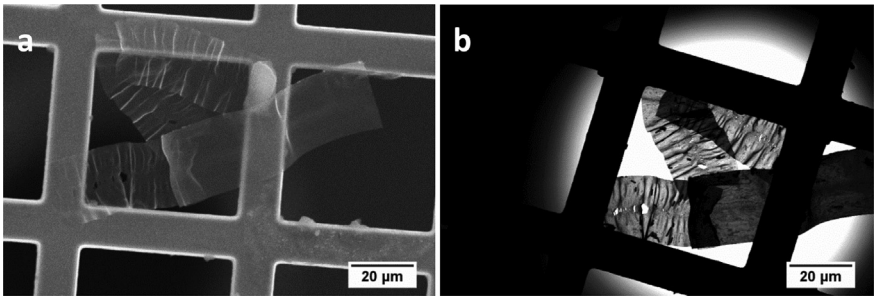

Fig. 2. Scanning electron micrographs in SE mode (a) and STEM mode (b) at very low magnification located at the ultramicrotomed sections on a copper supported grid. SE mode was used to identify the location of the titanium sections on the grid.

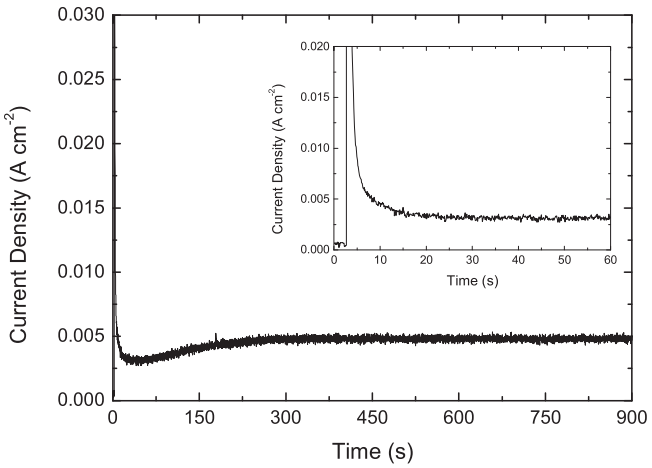

Fig. 3. Current density-time response for anodizing of titanium at 50 V in 1 M H_3PO_4 for 900 s at ambient temperature. The inset graph shows the initial stage of current density-time response up to 60 s.

created. STEM is a type of TEM operation; as with any transmission illumination scheme, the electrons pass through a sufficiently thin specimen. STEM focuses the electron beam into a narrow spot, which is scanned over the specimen in a raster [12]. Thus, the image created in the SE mode (Fig. 2a) is basically for identifying locations of the anodized titanium specimens; then, the STEM mode is used for further detailed information (Fig. 2b).

The current density − time response during anodizing at 50 V for 900 s is shown in Fig. 3. The magnified inset graph shows that the anodizing was initiated after ~2 s due to the operation delay; the current density decreased rapidly from an initial relatively high value after the time of ~3 s. The significant current drop was reduced gradually after ~10 s, which corresponded to the growth of a barrier oxide layer on titanium in the phosphoric acid. After ~75 s, the current density slightly increased, followed by a steady status of the current since ~150 s, is revealed. A current density of ~5.0 × 10^{-3} A cm^{-2} was maintained at 900 s. The anodized sputtering titanium in the Inlens and SE modes is shown in Fig. 4a and Fig. 4b respectively. The titanium layer and the anodic film are not distinguishable, except that the aluminium substrate can be observed. One of the details obtained from the scanning transmission electron micrograph (Fig. 4c) is the thickness of the anodic film, 100 ± 10 nm is revealed as a growth rate of ~2 nm V^{-1}. The oxygen bubbles present within the anodic films can be also observed within a size range ~5–30 nm. It is displayed that the film thickness, and the oxygen bubbles originated from oxygen evolution occurred during anodizing, probed routinely by TEM, can also be characterized using the STEM-in-SEM mode, and the image contrast is better than the Inlens and SE modes in SEM. Further, the large field at flexible magnification ranges from very low to very high, is also an important advantage for the STEM-in-SEM. At a relatively low magnification (79 kX), the uniform anodic

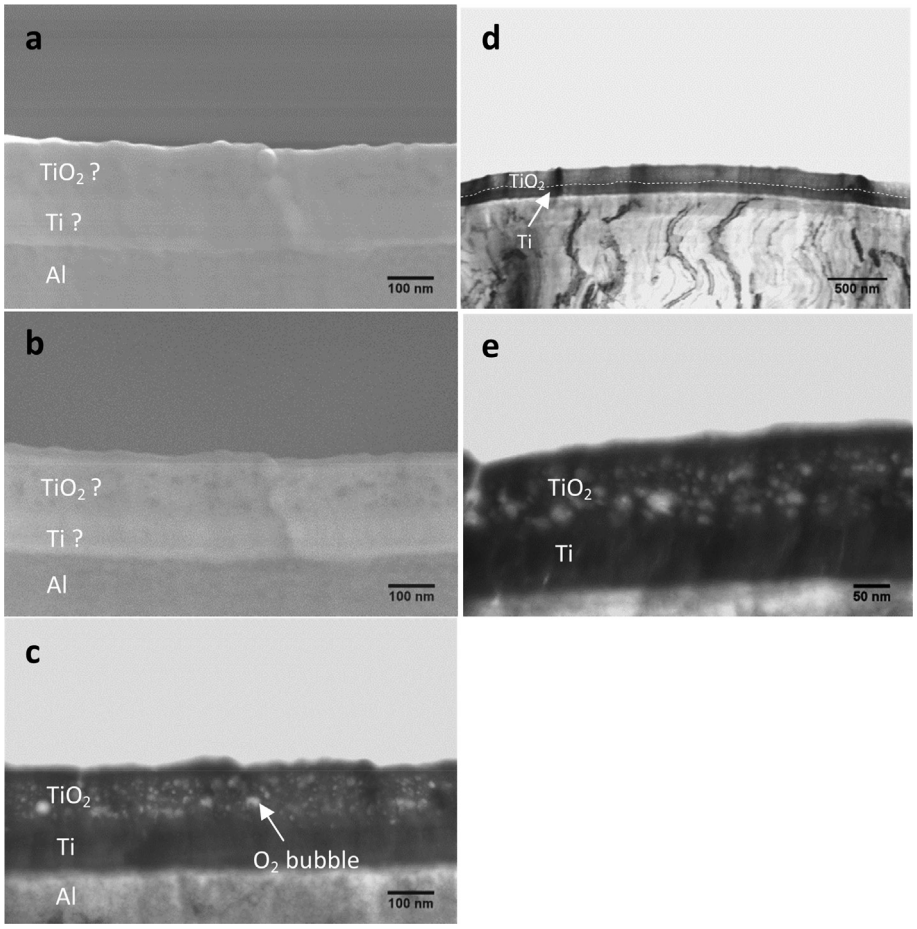

Fig. 4. Scanning electron micrographs at different modes and different magnifications of anodic oxide film formed on sputter-deposited titanium after potentiostatic anodizing at 50 V in 1 M H_3PO_4 for 900 s at ambient temperature, a magnification at 306 kX for a), Inlens mode, b), SE mode and c), STEM mode; d), a lower magnification at 79 kX in STEM mode and e), a higher magnification at 500 kX in STEM mode.

oxide film formed on the sputter-deposited titanium can be observed (Fig. 4d). At a relatively high magnification (500 kX), the feature of the development of oxygen bubbles within the film is shown clearly. Moreover, the findings from the STEM-in-SEM observation confirm that the amorphous-to-crystalline transition occurred during film growth on titanium in the phosphoric acid electrolyte during the initial stages of anodizing, and the nucleation of nanocrystals was induced, producing an increase in electron conduction [13]. Further, oxygen-filled voids were developed in the different regions of the oxide film, and the bursting of the oxygen gas due to the unbalance between the internal pressure and the electrostriction force would trigger the rupture of the anodic oxide film and lead to the formation of oxygen bubble features. Such findings are consistent with previous studies [13–17]. On the other hand, it has been reported [13] that anodizing could be operated with a combination of potentiodynamic and potentiostatic polarizations instead of applying a constant voltage directly; consequently, it would be interesting to use the STEM-in-SEM technique to investigate such anodic oxide films formed on titanium for the requirement of the fast speed analysis in the future.

The main highlight of STEM-in-SEM over TEM is its suitability as the ideal equipment for environments that demand rapid morphological analysis of specimens in large numbers at low cost. Such is the case in a typical production environment of anodic coatings on titanium, where morphological parameters can be monitored and critically controlled as quality control factors in the manufacturing processes as well as research purposes. Practically, extensive morphology analysis to such an extent is not carried out even in the most advanced processing plants, since it indeed is not carrying out TEM analysis in large numbers and with rapid turnaround. However, the situation can be simplified using STEM-in-SEM. As found earlier, it is possible to conduct high throughput by STEM-in-SEM imaging in an industrial environment. In such work, the single-specimen STEM has been re-designed to embrace a carousel system, which can handle up to 6 specimens simultaneously. The throughput of the system is therefore considerably higher than a TEM, or an STEM using a conventional single specimen holder. Most of the commercial SEM suppliers now offer STEM as an attachment, with the capability to handle up to six specimens or more. The use of the multi-specimen carousel has enabled remarkably higher equipment productivity and better utilization of operator time.

The estimation of the time saving from deployment of the STEM-in-SEM carousel in comparison with a single-specimen system was derived from careful analysis of the steps involved in the STEM-in-SEM process, and comparison with a TEM. Steps involved can be divided into the following two main stages; (1) specimen preparation involves the standard ultramicrotomy approach to prepare TEM sections; and (2) imaging involves loading the specimen holder into the microscope, STEM-in-SEM unit on the SEM specimen holder, evacuating the chamber until the required vacuum level is achieved, locating the region of interest and acquiring images of relevant features and, finally, removing the specimen. While both steps are common for TEM and STEM-in-SEM, but were optimized in terms of speed and quality, major differences were shown in productivity which was estimated between the two techniques when the 6-specimen carousel holder was designed for the STEM-in-SEM. It is estimated that the time saving per specimen resulted in a 20% increase in imaging productivity compared with TEM imaging. An added benefit of the carouse holder is that it contributes to increasing the lifetime of the equipment by limiting the number of occurrences of pumping and venting cycles, and by limiting filament warm-up for TEM.

An STEM-in-SEM system with a 6-specimen carousel allows straightforward analysis of the anodic oxide film coatings on titanium in terms of quality of information, with a remarkable improved speed of analysis. This makes the STEM-in-SEM a very practical and affordable alternative to TEM analysis, especially in industrial environments for the morphology characterization of anodic coatings. Further, STEM-in-SEM provides imaging at a large field with flexible magnification ranges from very low to very high. Therefore, the whole anodic film thickness generated on titanium, the crystalline structure and the oxygen bubble features originating from the oxygen evolution during anodizing can be clearly identified and analyzed by the STEM-in-SEM technique.

Acknowledgements

The authors are grateful to the Engineering and Physical Sciences Research Council (UK) for support of the LATEST 2 Programme Grant.

References

[1] Yetim AF. Investigation of wear behavior of titanium oxide films, produced by anodic oxidation, on commercially pure titanium in vacuum conditions. Surf Coatings Technol 2010;205:1757–63.
[2] Yetim AF, Yildiz F, Vangolu Y, Alsaran A, Celik A. Several plasma diffusion processes for improving wear properties of Ti6Al4V alloy. Wear 2009;267:2179–85.
[3] Yetim AF, Alsaran A, Efeoglu I, Çelik A. A comparative study: the effect of surface treatments on the tribological properties of Ti–6Al–4V alloy. Surf Coatings Technol 2008;202:2428–32.
[4] Smith CL, L MR, MacKenzie M. New opportunities for nanomineralogy using FIB, STEM/EDX and TEM. Microsc Analysis 2006;111:17–20.
[5] Nakagawa M, Dunne R, Koike H, Sato M, Pérez-Camacho JJ, Kennedy BJ. Low voltage FE-STEM for characterization of state-of-the-art silicon SRAM. J Electron Microsc 2002;51:53–7.
[6] Russias J, Frizon F, Cau-Dit-Coumes C, Malchère A, Douillard T, Joussot-Dubienz C. Incorporation of aluminum into C–S–H structures: from synthesis to nanostructural characterization. J Am Ceram Soc 2008;91:2337–42.
[7] Acevedo-Reyes D, Perez M, Verdu C, Bogner A, Epicier T. Characterization of precipitates size distribution: validation of low-voltage STEM. J Microsc 2008;232:112–22.
[8] Brown GM, Westwood AD. Characterization of polymers and catalysts using scanning transmission electron microscopy (STEM) in a field emission SEM. Microsc Microanal 2003;9:1020–1.
[9] Lee MR, Smith CL. Scanning transmission electron microscopy using a SEM: applications to mineralogy and petrology. Mineral Mag 2006;70:579–90.
[10] Coyne E, Magee JP, Mannion P, O'Connor GM, Glynn TJ. STEM (scanning transmission electron microscopy) analysis of femtosecond laser pulse induced damage to bulk silicon. Appl Phys A 2005;81:371–8.
[11] Paredes AM. Microscopy|scanning electron microscopy. In: Tortorello CABL, editor. Encyclopedia of food microbiology. 2nd ed. Oxford: Academic Press; 2014. p. 693–701.
[12] Keyse R, AJG-R, Goodhew PJ, Lorimer GW. Introduction to scanning transmission electron microscopy. Bios Scientific Publishers; 1998.
[13] Mazzarolo A, Curioni M, Vicenzo A, Skeldon P, Thompson GE. Anodic growth of titanium oxide: electrochemical behaviour and morphological evolution. Electrochim Acta 2012;75:288–95.
[14] Habazaki H, Takahiro K, Yamaguchi S, Shimizu K, Skeldon P, Thompson GE, et al. Influence of tungsten species on the structure of anodic titania. Philos Mag A 1998;78:171–88.
[15] Habazaki H, Uozumi M, Konno H, Shimizu K, Nagata S, Asami K, et al. Influences of structure and composition on growth of anodic oxide films on Ti Zr alloys. Electrochim Acta 2003;48:3257–66.
[16] Habazaki H, Uozumi M, Konno H, Shimizu K, Nagata S, Asami K, et al. Influence of molybdenum species on growth of anodic titania. Electrochim Acta 2002;47:3837–45.
[17] Habazaki H, Uozumi M, Konno H, Shimizu K, Skeldon P, Thompson GE. Crystallization of anodic titania on titanium and its alloys. Corros Sci 2003;45:2063–73.